

常温空气无焰燃烧在燃煤锅炉 煤改气中的应用

邢献军, 王宝源, 林其钊

(中国科学技术大学 热科学和能源工程系, 安徽 合肥 230026)

摘 要: 在燃煤锅炉的炉膛内安装常温空气无焰燃烧反应器, 可将燃煤锅炉改造为燃气锅炉。计算表明: 与其它燃气锅炉以对流换热为主的热交换方式不同, 该锅炉强化炉内换热, 辐射换热热量提高。实测结果: 锅炉热效率达到 92.92%, 比改造前提高 30% 以上, 比现有同吨位的燃气锅炉高 4% 以上。由于锅炉实现了无焰燃烧, 反应器温度分布均匀, 尾气污染物排放远低于国家标准。

关 键 词: 燃煤锅炉; 常温空气无焰燃烧; 煤改气; 高效; 减排

中图分类号: TK229.8 文献标识码: A

前 言

在锅炉设计中, 燃煤锅炉的炉内热强度低于燃气锅炉的炉内热强度, 因而同吨位的燃煤锅炉炉膛容积是燃气锅炉的 3~4 倍。将燃煤锅炉改造为燃气锅炉, 宽大的炉膛为燃气的燃烧提供了足够的空间, 锅炉设计的辐射受热面积和对流受热面积满足燃气锅炉所需的受热面积。但燃气燃烧反应速度快, 燃烧所释放的能量如得不到及时的吸收, 将会随烟气排放到大气中。因而, 将燃煤锅炉改造为燃气锅炉后, 提高锅炉热效率的最有效方法是增大炉膛的热辐射量, 而燃煤锅炉炉膛的独特结构, 提供了较大的锅炉受热面可以接受辐射热, 这为锅炉煤改气后提高炉膛辐射换热热量提供了条件。常温空气无焰燃烧技术的实现, 在炉膛内安装无焰燃烧反应器, 利用反应器高温辐射壁, 可以增大炉膛的热辐射量, 为燃煤锅炉改造为燃气锅炉提供了技术支持。

1 实 验

实验是在一台 KZL2-0.68-A2 型燃煤锅炉中进行的。在不改动炉膛内锅筒、水冷壁管布置的前

提下, 撤除炉膛内的炉排和前后拱, 安装一个特别设计的 2.0 MW 同轴射流燃烧器和一个几何尺寸为 W 1000 mm、 H 1000 mm、 L 3000 mm 的燃烧反应器。燃烧反应器两侧和顶部采用导热材料(该材料荷重软化温度高于 2000 °C, 并且不氧化, 使用寿命长), 导热系数为 23 W/(m·K)(当温度为 1200 °C 时), 燃烧反应器外用于稳定受热的锅筒和水冷壁管外壁温度设为 453 K(蒸汽压力为 0.4 MPa)。燃烧反应器底部和前后两端, 均采用绝热材料(见图 1)。控制系统按燃气锅炉设计要求执行。用热值为 35.8 MJ/m³ 的天然气为燃料。

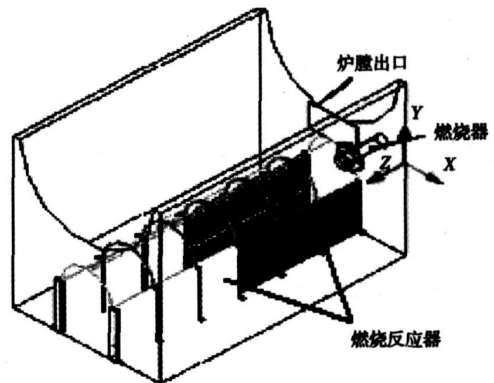


图 1 KZL2-0.68-A2 型锅炉炉膛改造

改造后, 炉膛内的能量传递由 3 部分组成:

(1) 燃烧反应器辐射壁通过辐射传热给锅筒和水冷壁管。

(2) 高温烟气通过对流传热给锅筒、水冷壁管和锅筒内烟管。

(3) 炉墙通过辐射传热给水冷壁管。

因天然气在燃烧反应器内进行燃烧, 从燃烧反应器内排出的烟气主要成份是 CO₂、H₂O 和 N₂, 燃煤

锅炉改成燃气锅炉后,在锅炉对流受热面传热计算中忽略烟气的辐射换热。

将常温空气和天然气按照扩散燃烧的方式,分别从燃烧器出口送入炉膛。在启动过程中,炉膛温度较低,燃烧反应器内为传统的有焰燃烧方式;当天然气流量 G 增大为 $100 \text{ m}^3/\text{h}$ 时,火焰消失,炉膛内透明,形成了看不见火焰的无焰燃烧,图2是从燃烧器对面拍摄的炉膛内的无焰燃烧照片。实验工况条件见表1。

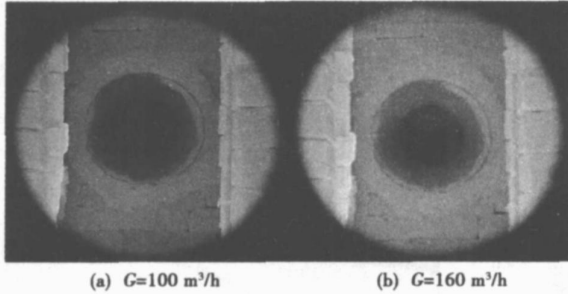


图2 炉膛内无焰燃烧照片

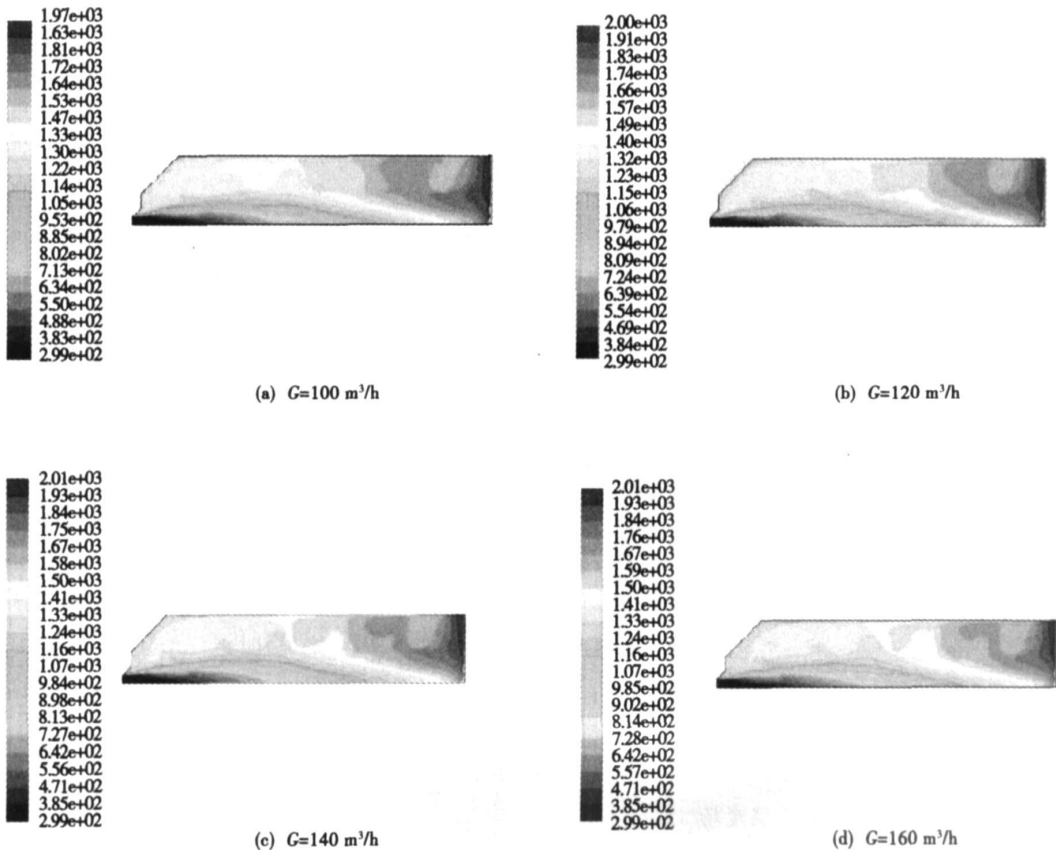


图3 不同天然气流量下的炉内温度分布状况($\alpha=1.05$)

表1 不同工况燃烧反应的实验条件

天然气流量 $G/\text{m}^3 \cdot \text{h}^{-1}$	过量空气系数 α		
100	1.02	1.05	1.10
120	1.02	1.05	1.10
140	1.02	1.05	1.10
160	1.02	1.05	1.10

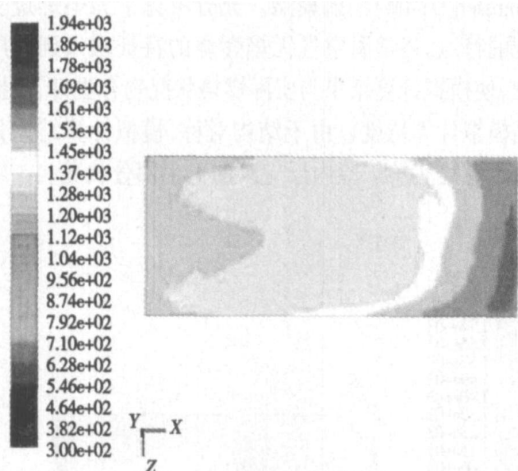
2 燃烧反应器内温度场研究

2.1 数值模拟计算

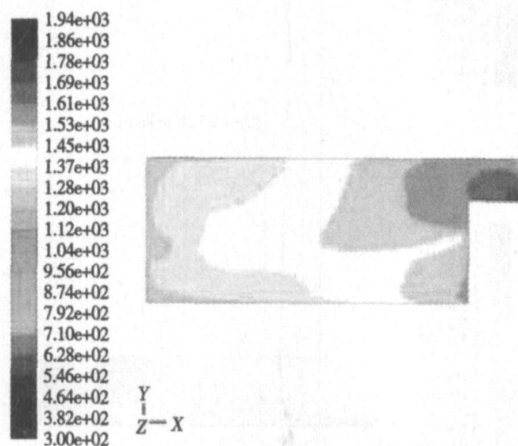
使用 Fluent 商业软件对不同工况燃烧反应的实验进行模拟计算^[1,11]。在计算过程中,速度压力耦合方程采用 SIMPLE 算法,并且选择了非预混燃烧模型的 PDF 方法、准雷诺应力粘性模型、Discrete Transfer [DTRM] 辐射模型。充分考虑了无焰燃烧实现的特点,将常温空气无焰燃烧的特征融入到程序中,使模拟计算结果与实际燃烧状况吻合更好,以提高模拟计算精度。由于结构对称,模拟计算结果只显示燃烧实验炉膛内反应区的上半部分状况。

图3显示在不同天然气流量下的炉内温度分布状况。在燃烧器气体射流的对称轴上,随着离开喷口的距离增加,温度急剧上升,在燃烧器喷口处,温度最低,燃料与空气温度接近环境温度,离喷口2 000 mm处温度立即升高到1 000 ℃以上。在燃烧器射流对称轴上,温度较低,反应强度较弱,在 $\phi 300 \times 2\,000$ mm柱状空间以外,温度均在1 000 ℃以上,且温差相差不大,说明在柱状空间外燃烧反应强度基本相同。近辐射壁处的温度均在1 200 ℃以上。不断增大炉膛内的容积热负荷,以提高锅炉的吸热量。当天然气流量G达到160 m³/h时,不再增大天然气流量,辐射壁内表面温度分布见图4。根据温度场可以算出:燃烧反应器顶部辐射壁内表面平均温度约为1 203 ℃,两侧辐射壁内表面平均温度约为1 205 ℃。

上显示的温度比较,同一工况下同一点的温度,实测的温度比计算的温度均要高5~20 ℃,且温度变化趋势相同。燃烧器喷口中心射流轴线方向上温度曲线显示温度上升较快,温度梯度大,说明炉膛中心燃烧器射流对称轴线上混合扩散过程剧烈;炉内近两侧炉壁沿射流轴线方向上的温度曲线比较平缓,温度梯度小,说明炉膛四周的温度比较均匀,燃烧强度弱,也就是说,形成无焰燃烧后,炉膛四周温度场是均匀的,燃烧稳定,这与高温空气无焰燃烧特性是一致的^[2~4];因炉膛后墙绝热,则在炉膛后部有很小的高温区,温度梯度大。与高温空气无焰燃烧特性不同的是,燃烧器喷口射流对称轴线上温度较低。随着天然气流量的增大,实测的各点温度均有所上升。



(a) 顶部辐射壁



(b) 两侧辐射壁(缺口处为反应气出口)

图4 辐射壁表面温度场

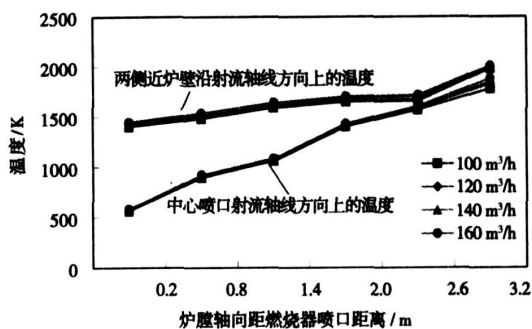


图5 燃烧器喷口射流轴线方向上的温度变化($\alpha=1.05$)

实测的燃烧反应器顶部辐射壁表面平均温度为1 227 ℃,两侧辐射壁表面平均温度为1 200 ℃,烟气温度为1 350 ℃。模拟计算的壁温为燃烧反应器辐射壁内表面温度,而实测的壁温为燃烧反应器辐射壁外表面温度,两者存在误差,误差约为1.6%,说明计算模型的建立是比较符合实际的。

从图5可以看出:因为炉膛后部绝热,所以存在部分高温区;从整个辐射面的温度分布可以看出:温度分布比较均匀,温差不大,辐射面表面温度高,将使热辐射量增大。将此燃烧反应器安装在炉膛内,对提高锅炉热效率是有利的。

3 锅炉热效率计算^[5~10]

3.1 实际测试数据

- 锅炉房环境温度: 21 ℃
- 锅炉炉墙温度: 36 ℃(平均)
- 锅炉排烟温度: 140 ℃
- 锅炉炉膛温度: 1 350 ℃

2.2 实测值与模拟值的比较

图5为实验测得的炉膛内温度。同模拟计算图

锅炉进水温度: 13 ~ 20 °C

每产生 1 t 0.4 MPa, 151 °C 的水蒸气消耗天然气 80.46 m³

3.2 计算结果

3.2.1 锅炉有效吸热量

1 t 0.4 MPa 的水由 16.5 °C 升高到 151 °C 的吸热量为:

$$Q_1 = (2747.5 - 69.7) \times 10^3 = 2.678 \times 10^6 \text{ kJ}$$

3.2.2 进入锅炉的总能量

天然气的总发热量为 $3.58 \times 10^4 \text{ kJ/m}^3$, 80.46 m³ 天然气的总发热量为:

$$Q_0 = 80.46 \times 3.58 \times 10^4 = 2.882 \times 10^6 \text{ kJ}$$

3.2.3 锅炉效率

根据能量平衡理论, KZL2-0.68-A2 煤改气锅炉的效率为:

$$\eta = Q_1 / Q_0 = 92.92\%$$

4 锅炉烟气中污染物浓度测试

测试数据见表 2。

表 2 烟气测试成份 ($\alpha = 1.05$)

测试项目	测试结果
烟尘	16.2 mg/m ³
SO ₂	< 2.86 × 10 ⁻⁶
NO _x	90 × 10 ⁻⁶
CO	8 × 10 ⁻⁶
CO ₂	9.3%
C _x H _y	未检出

测试数据显示: 燃煤锅炉改烧天然气后, 天然气的燃烧效率几乎达到 100%, 尾气中不含硫化物, NO_x 浓度为 90 × 10⁻⁶, 烟尘为 16.2 mg/m³, CO 浓度为 8 × 10⁻⁶。所有排放指标都远低于国家关于《锅炉大气污染物排放标准》中规定的燃气锅炉排放指标: 烟尘小于 50 mg/m³, SO₂ 小于 100 × 10⁻⁶, NO_x 小于 400 × 10⁻⁶。特别是 NO_x 的排放远远低于现有燃气锅炉排放水平, 这将对解决天然气锅炉的 NO_x 污染, 具有十分重要的意义。

5 结论

(1) 无焰燃烧反应器, 可促进燃烧反应, 强化炉内换热过程, 降低锅炉对燃烧器的要求, 能够起到稳定火焰的作用。

(2) 实测结果: 锅炉热效率达到 92.92%, 与原燃煤时锅炉的热效率相比, 提高 30% 以上, 比现有同吨位的燃气锅炉热效率高。

(3) 改造后的燃气锅炉由于实现了无焰燃烧, 在过量空气系数为 1.05 时, 烟气中 NO_x 浓度为 90 × 10⁻⁶, 排烟中 CO 浓度为 8 × 10⁻⁶, 尾气污染物排放远低于国家关于《锅炉大气污染物排放标准》中规定的燃气锅炉排放指标, 在建设资源节约型和环境友好型社会中的效益尤为突出。

(4) 改造后的燃气锅炉, 因在炉膛内安装无焰燃烧反应器, 炉膛内温度场均匀, 且锅炉受压部件不直接与火焰接触, 将使锅炉应力分布均匀, 容积热负荷高, 减缓材料氧化速度, 运行更加安全可靠, 延长锅炉使用寿命。

参考文献:

- [1] ZHU T, ZHANG Y M, LIU M F, et al. Numerical simulation of high temperature combustion for low heat value gas[J]. Journal of Tongji University, 2002, 30(8): 932-937.
- [2] CAVALIERE A, DE JOANNON M. Mild combustion[J]. Prog Energy and Combust Sci, 2004, 30: 329-366.
- [3] MILANI A, SAPONARO A. Diluted combustion technologies[J]. The IFRE Electronic Combustion Journal, 2001(1): 1-32.
- [4] KATSUKI M, HASEGAWA T. The science and technology of combustion in highly preheated air[J]. Proc Combust Inst, 1998, 27: 3135-3146.
- [5] 范从振. 锅炉原理[M]. 北京: 中国电力出版社, 1986.
- [6] 冯俊凯, 沈幼庭. 锅炉原理及计算[M]. 第二版. 北京: 科学出版社, 1992.
- [7] 林宗虎. 锅炉实用手册[M]. 北京: 化学工业出版社, 1999.
- [8] 宋贵良. 锅炉计算手册[M]. 沈阳: 辽宁科学技术出版社, 1995.
- [9] 钟 威, 许跃敏, 董水光. 通用锅炉热力计算算法研究[J]. 工业锅炉, 2000(2): 24-27.
- [10] 郭宽良. 计算传热学[M]. 合肥: 中国科学技术大学出版社, 1988.
- [11] YUAN J W, NARUSE I. Effects of air dilution on highly preheated air combustion in a regenerative furnace[J]. Energy and Fuels, 1999, 13(1): 99-104.

(编辑 何静芳)

el coal PM₁₀. By using the above algorithm, simulated was the aggregation dynamics process of fly-ash fine particles in a uniform magnetic field, which have been produced during the combustion of Dongsheng-origin bituminous coal. A comparison of the simulation results with the test ones shows a complete correspondence between the two results. The dual-subregion algorithm features a relatively good applicability. For particle diameters ranging from 0.023 to 9.318 μm, the aggregation and removal efficiency of the intermediate-sized particles is higher than that of small and large-sized particles. An enhancement of the following factors, i. e. magnetic induction intensity of an outer magnetic field, particle total mass concentration, residence time of particles in the magnetic field and gas flow average velocity, can increase the aggregation and removal efficiency of the particles. After the particles have attained saturation magnetization, the intensification of the outer magnetic field will have no influence on particle aggregation. When the product of the gas flow average velocity and the residence time of the particles in the magnetic field is a constant, the aggregation and removal efficiency of the particles will decrease with an increase of gas flow average velocity. The particle size corresponding to a maximal particle-size-based removal efficiency of the particles and the particle-number median diameter will decrease with an increase of the aggregation-related total removal efficiency. **Key words:** fuel coal PM₁₀, magnetic aggregation, dual-subregion algorithm, ash removal efficiency

燃煤 PM₁₀在高梯度磁场中的捕集 = **Capturing of Fuel Coal PM₁₀ in a High Gradient Magnetic Field** [刊, 汉] / LU Duan-feng, WU Xin, ZHAO Chang-sui, et al (Education Ministry Key Laboratory on Clean Coal Power Generation and Combustion Technology under the Southeast University, Nanjing, China, Post Code: 210096) // Journal of Engineering for Thermal Energy & Power. — 2007, 22(3). — 280 ~ 283

According to the high-gradient magnetic separation theory and with the magnetic field, flow field, Brown diffusion and inertia action being taken into account, a model for capturing inhalable particles of fuel coal in a high-gradient magnetic field has been established along with a calculation of the capturing efficiency of particles. A contrast-based analysis of the calculation results and the test ones indicates that for the particle diameters ranging from 0.023 μm to 9.3 μm, the calculated value of the capturing efficiency of particles assumes a basically identical tendency as the test one and for the particle diameters ranging from 1 μm to 9.3 μm, the calculated value is in relatively good agreement with the test one with the error being less than 5%. A relatively high particle magnetized intensity, magnetic field intensity and relatively long residence time can all be favorable to the capture of particles in the magnetic field. The Brown diffusion plays a relatively strong contributory role in enhancing the efficiency of capturing particles having a diameter of less than 1 μm while the inertia action has a weak influence on particle capturing efficiency. The research results indicate that using a high gradient magnetic field to capture fuel-coal-produced inhalable particles is a valid and feasible approach. **Key words:** fuel coal PM₁₀, high gradient magnetic field, numerical simulation

常温空气无焰燃烧在燃煤锅炉煤改气中的应用 = **Application of Flameless Combustion at a Normal Air Temperature for a Coal-fired Boiler Being Converted to Burn Gas** [刊, 汉] / XING Xian-jun, WANG Bao-yuan, LIN Qi-zhao (Department of Thermal Science and Energy Source Engineering, China National University of Science and Technology, Hefei, China, Post Code: 230026) // Journal of Engineering for Thermal Energy & Power. — 2007, 22(3). — 284 ~ 287

By installing a flameless combustion reactor operating at a normal-air temperature in the furnace of a coal-fired boiler it is possible to convert a coal-fired boiler into a gas-fired one. Relevant calculation results show that as different from the predominant convection heat-exchange mode adopted by other gas-fired boilers, the furnace of the gas-fired boiler under discussion assumes mainly a radiation heat-exchange mode, thus intensifying in-boiler heat exchange. The actual measurement results indicate that a boiler thermal efficiency of 92.92% can be attained, over 30% higher than that of the boiler before modification and more than 4% higher than that of boilers with the same capacity currently available. As the boiler

has realized a flameless combustion and the reactor has a uniform temperature distribution, the pollutant emission level of exhaust gases is far lower than that set by the applicable national standard. **Key words:** flameless combustion at a normal air temperature, coal-fired boiler being converted to burn gas, high efficiency, reduction of emissions

链条炉横向配风不均匀性的研究= **An Investigation of the Non-uniformity of Transversal Air Distribution for a Chain Grate Stoker** [刊, 汉]/CHANG Bin, YU Ya-hui, JI Jun-jie, et al (Thermal Energy Engineering Research Institute under the Shanghai Jiaotong University, Shanghai, China, Post Code: 200240)// Journal of Engineering for Thermal Energy &Power. — 2007, 22(3). — 288 ~ 291

The non-uniformity of transversal air distribution in a chain grate stoker can seriously affect the stoker efficiency. To solve this problem, real stoker cold-state tests have been performed of the air supply system of a 20 t/h chain grate stoker in 7 operating regimes. The test results show that the unsatisfactory lateral seal of the grate and air damper deformation are the main causes leading to the non-uniformity of air distribution. With the actually measured data serving as boundary conditions, a numerical simulation was conducted of air flow in a single wind box by employing a $k-\epsilon$ turbulence model. It has been found that the diffusion-flow pressure drop and a conversion from a kinetic pressure to a static one as well as a turbulence perturbation in the wind box can cause the non-uniformity of transversal air distribution. In the light of the respective merits of large-air-box and small-air-funnel air supply system developed in China and underfeed air supply mode of foreign-made incinerators, proposed was an air supply system incorporating an underfeed large-air-box and small-air-funnel. A numerical simulation of the above two kinds of air supply system indicates that the improved air supply system can effectively enhance the uniformity of transversal air distribution. **Key words:** chain grate stoker, cold state test, transversal air distribution, numerical simulation

燃煤电站锅炉高温腐蚀特征的研究= **A Study of High-temperature Corrosion Characteristics of Coal-fired Utility Boilers** [刊, 汉]/GAO Quan, ZHANG Jun-ying, QIU Ji-hua, et al (National Key Laboratory on Coal Combustion under the Central China University of Science and Technology, Wuhan, China, Post Code: 430074)// Journal of Engineering for Thermal Energy &Power. — 2007, 22(3). — 292 ~ 296

By adopting a variety of microscopic analytic methods, such as metallographic microscope and X-ray diffraction analysis, X-ray fluorescent probe analysis, electronic microscope-energy spectrum analysis by field emission scanning and aperture testing etc., a systematic analysis was conducted for the corrosion products of the water wall of a coal-fired utility boiler. The results of the analysis show that the corrosion products assume a laminar structure with its outer layer being loose and porous and its inner layer rather compact. The corrosion products mainly consist of iron sulfide, iron oxide and a small quantity of silicate. The element distribution regularity of the corrosion products from inside to outside can be given as follows: the content of silicon and aluminium assumes an ascending tendency and that of sulfur and iron a descending tendency. The mineral matter mainly includes iron sulfide and iron oxide generated by corrosion as well as silicon aluminate which originated from fly-ash particles. A comprehensive analysis of the composition and microscopic characteristics shows that the corrosion of the water wall pertains to one of sulfide type. **Key words:** high temperature corrosion, water wall, microscopic structure, X-ray diffraction, coal combustion

基于自抗扰的多变量解耦控制在球磨机的应用= **Application of an Auto-disturbance-rejection-controller-based Multivariable Decoupling Control in Ball Mills** [刊, 汉]/MA Yong-guang, HAO Na, LI Peng-fei, et al (College of Control Science and Engineering under the North China University of Electric Power, Baoding, China, Post Code: 071003)// Journal of Engineering for Thermal Energy &Power. — 2007, 22(3). — 297 ~ 300

A ball mill-based milling system in a thermal power plant is a typical three-input and three-output system. There is a se-